

Glucose Utilization In Vivo by Human Pulmonary Neoplasms

KEITH B. NOLOP, MD, CHRISTOPHER G. RHODES, MSc, LARS H. BRUDIN, MD, RONALD P. BEANEY, MRCP, THOMAS KRAUSZ, MRCPATH, TERRY JONES, DSc, AND J. M. B. HUGHES, FRCP

Neoplastic tissue in general shows a high rate of glucose consumption under both anaerobic and aerobic conditions. Using positron emission tomography (PET) we measured the rate of uptake of the glucose analogue ^{18}F fluoro-2-deoxy-D-glucose (^{18}FDG) in 12 patients with carcinoma of the lung. The tumor types were six squamous cell, two large cell, two oat cell, one adenocarcinoma, and one undifferentiated carcinoma. In each patient a transaxial plane was selected that contained the bulk of the tumor tissue. Regional density and blood volume were measured. Following the intravenous injection of ^{18}FDG , the rates of uptake in the tumor and normal lung tissue were assessed from sequential scans over 1 hour. In each patient the rate of uptake of ^{18}FDG in the tumor tissue was significantly increased relative to normal lung tissue. For the group the rate of uptake by the tumor was 211.4 ± 69.4 ml/100 g/hr (mean \pm SD) compared to 31.9 ± 13.2 in the contralateral lung ($P < 0.05$). The tumor-to-normal tissue ratio of 6.6 (range, 2.7 to 14.6) was higher than previously reported ratios for brain and liver tumors. In contrast to brain tumors there was little correlation between tumor type and rate of ^{18}FDG uptake. Measurements of glucose metabolism taken *in vivo* in human pulmonary tumors may lead to advances in screening, staging, and therapy.

Cancer 60:2682-2689, 1987.

THIRTY YEARS AGO, Warburg demonstrated abnormal glucose metabolism in neoplastic tissue *in vitro*.¹ Compared to normal hepatic tissue, rapidly growing, poorly differentiated hepatic tumors showed increased glycolysis and lactate production despite the presence of abundant oxygen, resulting in high rates of glucose consumption. The mechanism of this increased glucose consumption probably depends on the type of tissue and may be due to increased glucose transport through the cell membrane² or an enhanced capacity for glycolysis because of increased activity of the key glycolytic enzymes.³

This differential metabolic property of neoplastic tissue has been used by several investigators to detect malignancy. Recent studies have been performed using the

glucose analogue ^{18}F fluoro-2-deoxy-D-glucose (^{18}FDG). When injected intravenously, ^{18}FDG rapidly diffuses into the extracellular spaces throughout the body. It is then transported across cell membranes into the tissues and phosphorylated by hexokinase. Because of the modification of the molecule at the second carbon position, the ^{18}FDG is not catabolized further and remains metabolically trapped.⁴ The rate at which the tracer accumulates in the tissue is thus dependent on the combined transport and hexokinase activity of the cells.

The uptake of ^{18}FDG has been measured in several experiments using tumors from animals.^{5,6} Studies have also been performed in man using radioisotopic imaging and positron emission tomography (PET). For example, the rate of ^{18}FDG uptake in patients with brain tumors has been reported to correlate with the tumor grade.⁷ In a small study a high rate of ^{18}FDG uptake was measured in hepatic metastases from colon carcinomas.⁸

Glycolysis in lung neoplastic tissue has not been extensively assessed. In one preliminary study⁹ orally administered ^{11}C -glucose was used as a qualitative marker of neoplastic tissue. Investigators have more recently measured the rate of ^{18}FDG uptake in pulmonary tissue using PET scanning. The calculated metabolic rate of the uptake of glucose in normal pulmonary parenchyma appears to be low in the fasting state and is enhanced by feeding.¹⁰ Increased pulmonary uptake of ^{18}FDG has

From the MRC Cyclotron Unit and Departments of Medicine and Histopathology, Royal Postgraduate Medical School, Hammersmith Hospital, London W12 0HS, England.

Supported by a British-American research fellowship award from the American Heart Association and by the U. K. Medical Research Council.

The authors thank the technicians and chemists of the MRC Cyclotron Unit for their assistance with patient scanning and Vic Aber from the Department of Medical Physics for statistical advice.

Address for reprints: Keith B. Nolop, MD, Division of Pulmonary Medicine, B1308 Medical Center North, Vanderbilt University Medical Center, Nashville, TN 37232.

Accepted for publication June 9, 1987.

been reported in patients with active sarcoidosis and cryptogenic fibrosing alveolitis.¹¹ Preliminary semi-quantitative data are also available and suggest an increase in ¹⁸F¹⁸FDG uptake by lung tumors compared to normal tissue.¹²

A quantitative assessment of glucose utilization by pulmonary neoplastic tissue has important therapeutic implications. Using PET scanning, we measured the rate of ¹⁸F¹⁸FDG uptake in 12 patients with lung carcinomas, posing the following questions: 1) Is ¹⁸F¹⁸FDG uptake in lung neoplastic tissue increased to a similar degree as in tumors of other organs? 2) Does the rate of ¹⁸F¹⁸FDG uptake correlate with tumor type, viability, and degree of differentiation?

Patients and Methods

Patients

Twelve patients with pulmonary carcinomas documented by biopsy were studied; only one had any treatment prior to the scan. All subjects ate a light breakfast on the morning of the scan, which was performed between 10 AM and 4 PM. The project was approved by the Ethics Committee of the Hammersmith Hospital in London and the U. K. Administration of Radioactive Substances Advisory Committee. Informed consent was obtained from each patient.

Histologic Analysis

Histologic material from each patient was examined in detail, except for one patient from overseas, whose physicians provided an extensive pathologic report. The tissue analyzed included cells from needle aspiration, bronchial washings, bronchial biopsies, lymph nodes, and resected specimens. The tumors were categorized according to the World Health Organization classification system¹³; we emphasized the degree of differentiation.

Positron Emission Tomography (PET)

Each patient was studied in a supine position. Canulas were placed in the antecubital veins of both arms to make separate sites for injection and blood sampling. Scanning was performed using an ECAT-II Pet Scanner (EG and G Ortec, CTI Corporation, Knoxville, Tennessee). In the medium resolution mode this provides reconstructed images of a single transaxial plane with a spatial resolution of 1.7 cm full-width, half-maximum in each dimension. After the patient was positioned in the scanner, the ring source of ⁶⁸Ge/⁶⁸Ga was placed between the patient and detector. Using a recent chest radiograph or computerized tomographic scan as a guide for the selected plane, several test transmission

scans were recorded to locate the tomographic slice containing the bulk of the tumor. A 10-minute transmission scan was then performed. This provided measurements of regional density and a means for correcting emission data for tissue attenuation.¹⁴ The ring source was shielded, and approximately 4.5 mCi (range, 1.6 to 6.1 mCi) of ¹⁸F¹⁸FDG was injected as a 30-second constant infusion. Six 3-minute scans and 9 5-minute scans were taken. Frequent samples of venous blood were taken during the scans (at 30-second intervals initially, lengthening to 5-minute intervals). From these samples plasma and whole blood isotope concentrations were measured using a sodium iodide well counter calibrated against the PET scanner pixel element response. Three blood samples were also taken at 30-minute intervals to analyze glucose concentration with standard enzymatic techniques. After the ¹⁸F¹⁸FDG scans were completed, each patient inhaled approximately 8 mCi of ¹¹C carbon monoxide to label the red blood cell hemoglobin, and a final 10-minute emission scan was performed to obtain a measurement of regional blood volume. During this scan, three additional venous blood samples were taken to measure ¹¹CO concentration.

Reconstruction of the transmission and emission scans provided regional values of density (g tissue/cm³ thorax), sequential ¹⁸F¹⁸FDG concentrations within the tomographic slice (μ Ci ¹⁸F¹⁸FDG/cm³ thorax), and blood volume (ml blood/cm³ thorax). The latter was calculated from the ¹¹CO red cell scan after subtracting background ¹⁸F¹⁸FDG activity within the slice. A value of 0.9 for the regional-to-peripheral hematocrit ratio was used.¹⁵ The sequential blood samples and the blood volume scan provided a means of calculating the thoracic concentration of vascular ¹⁸F¹⁸FDG as a function of time following injection. These vascular background scans were then subtracted from the recorded ¹⁸F¹⁸FDG scans to provide sequential measurements of the thoracic concentration of extravascular ¹⁸F¹⁸FDG. From the regional distributions of blood volume and lung density, a scan of extravascular lung density was obtained (g extravascular lung tissue/cm³ thorax).¹⁴ This information enabled the regional thoracic concentration of extravascular ¹⁸F¹⁸FDG to be converted into regional extravascular lung tissue concentration (μ Ci ¹⁸F¹⁸FDG/g tissue), thereby taking into account the effects of lung inflation and gas content on the regional thoracic content of ¹⁸F¹⁸FDG.

Data Analysis

Using the information from the serial scans and blood samples, calculations were performed to obtain the rate of ¹⁸F¹⁸FDG uptake by tissue and the apparent ¹⁸F¹⁸FDG distribution volume (see the Appendix at the end of this article for a summary of the mathematical calculations).

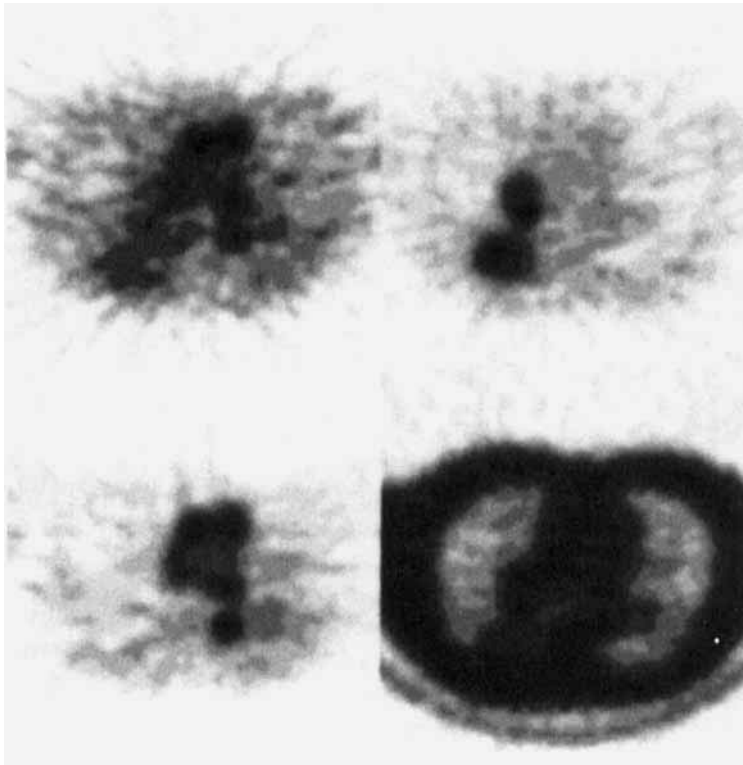


FIG. 1. Representative PET scans (Patient 4) are shown. Upper left = ^{18}F FDG accumulation at 3 min, upper right = ^{18}F FDG accumulation at 60 min, lower left = regional blood volume after ^{11}C CO inhalation, and lower right = regional density from the transmission scan.

These values were calculated on a pixel-by-pixel basis. For each patient separate regions of interest (ROI) were drawn for the neoplastic tissue, adjacent ipsilateral lung, contralateral lung, and contralateral chest wall, and the mean value within each region was calculated. The minimum size of any ROI was 7 cm^2 . A standard 4.5-cm^2 ROI was also used to determine the maximum ^{18}F FDG uptake within the tumor tissue. Data are presented as means \pm standard deviation. After logarithmic transformation of the data, comparisons were made using analysis of variance followed by testing for Fisher significant differences. A P value of <0.05 was considered to be statistically significant.

Results

Representative PET scans from Patient 4 are shown in Figure 1. Scans depicting the concentration of ^{18}F FDG at 3 and 60 minutes after injection are shown in the upper left and right pictures, respectively. Soon after the injection, the ^{18}F FDG was located mainly in the blood and extracellular spaces. One hour later, the ^{18}F FDG had concentrated within the tumor tissue as phosphorylated ^{18}F FDG.⁴ The lower left scan shows the regional blood volume obtained after ^{11}C CO inhalation. The lower right scan shows regional density obtained from the transmission scan.

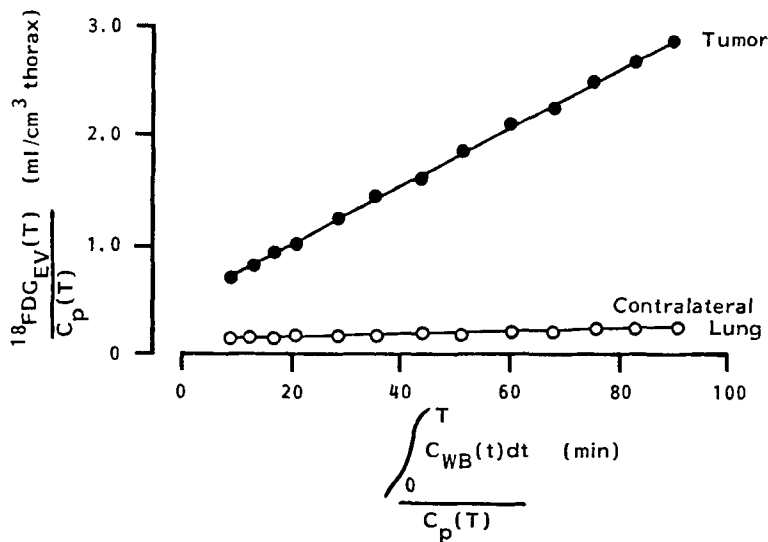
Figure 2 shows the progressive increase in the extravascular thoracic content of ^{18}F FDG in tumor and con-

tralateral lung for Patient 4. Both regions show a linear uptake, although the line for the tumor tissue has a much higher slope. The rate of ^{18}F FDG uptake is calculated as the slope of the line times 60 (to convert minutes to hours), which is then divided by the extravascular density within the region (see Appendix).

Table 1 summarizes for the 12 patients the histologic source material, location, and classification. Six patients had squamous cell carcinomas, two had large cell carcinomas, and two had oat cell carcinomas. Patient 11 had a lobectomy for adenocarcinoma 9 years prior to the scan and was scheduled to undergo radiotherapy for a suspected recurrence, although bronchial biopsy was negative for tumor. Patient 12 had a metastatic undifferentiated carcinoma documented in a cervical lymph node. Because of superior vena caval obstruction, she had been treated with radiotherapy to the mediastinum approximately 6 weeks prior to PET scanning.

Measured values of ^{18}F FDG uptake (mean and maximum), the coefficients of variation, and apparent ^{18}F FDG distribution volumes for the tumor and contralateral lung tissue are listed in Table 2. Eleven of the 12 tumors demonstrated a heterogeneous uptake as shown by the coefficients of variation; only Patient 8, who had a large cell carcinoma, had a low variability of ^{18}F FDG uptake. However, partial volume effects near the edge of each tumor limit the accuracy of the coefficient of variation as an index of intratumor variability. Patients 1, 3,

FIG. 2. Regional extravascular thoracic content of ¹⁸F DG increases with time (Patient 4). The ratio of extravascular thoracic content to plasma concentration (vertical axis) is plotted against cumulative exposure to vascular ¹⁸F DG in minutes (horizontal axis). The tumor tissue is shown by ●—●, and the contralateral lung tissue is shown by ○—○.



and 6, who had squamous cell carcinomas, showed areas of very low uptake within the mass that were consistent with necrosis. In these cases the ROI for the tumor tissue excluded the necrotic centers. There was no correlation between tumor location within the chest and ¹⁸F DG uptake. Likewise, there appeared to be little correlation between tumor type and rate of ¹⁸F DG uptake. In Patients 1, 2, 3, and 4, who had well-differentiated squamous cell carcinomas, the mean and maximum rates of ¹⁸F DG uptake were higher than in Patients 5 and 6, who had poorly-differentiated squamous cell carcinomas. Likewise, the four patients with higher grade tumor tissue (large cell anaplastic and oat cell carcinomas) had rates of ¹⁸F DG uptake that were not significantly different from the six patients with squamous cell carcinoma. However, the only patient with adenocarcinoma, Patient 11, had the lowest rate of ¹⁸F DG uptake. Patient 12, who had metastatic carcinoma of unknown origin and was treated with radiotherapy 6 weeks prior to the scan, had the highest rate of ¹⁸F DG uptake.

Figure 3 shows for the group the rates of ¹⁸F DG uptake (mean ± SD) by the tumor (211.4 ± 69.4 ml/100 g/hr), ipsilateral lung (50.0 ± 21.0), contralateral lung (31.9 ± 13.2), and chest wall (11.1 ± 2.4). In each patient ¹⁸F DG uptake by the tumor was significantly higher than either lung (*P* < 0.05), and the chest wall consistently showed the lowest uptake (*P* < 0.05). The mean value for the ipsilateral lung was higher than that of the contralateral lung (*P* < 0.05). The ratio of ¹⁸F DG uptake for tumor-to-contralateral lung was 6.6 for the 12 patients, ranging from 2.7 (Patient 5) to 14.6 (Patient 3), both of whom had squamous cell carcinomas.

The calculated volumes of distribution are shown in Figure 4. Values for the ipsilateral lung (58.2 ± 11.6 ml/100 g) and contralateral lung (53.1 ± 11.8) are simi-

lar, but both are significantly greater than tumor tissue (44.0 ± 13.4) and chest wall (16.4 ± 4.3), (*P* < 0.05).

Discussion

This study confirms that lung carcinomas, like tumors of other tissues, have a high rate of uptake of the glucose analogue ¹⁸F DG. Moreover, the ratio of tumor uptake to normal lung tissue uptake, 6.6, is higher than corresponding ratios for other neoplasms in man. Brain

TABLE 1. Histologic Information

Patient	Age	Sex	Histologic source	Tumor location	Classification
1	81	M	Needle aspirate	Apex	WD squamous carcinoma
2	62	M	Needle aspirate	Midlung	WD squamous carcinoma
3	75	M	Needle aspirate	Upper lobe	WD squamous carcinoma
4	64	M	Paratracheal node	Lower lobe	WD squamous carcinoma
5	72	M	Bronchoscopy	Apex	PD squamous carcinoma
6	69	F	Bronchoscopy	Lower lobe	PD squamous carcinoma
7	72	M	Bronchoscopy	Mainstem	Large cell carcinoma
8	51	F	Cervical node	Lower lobe	Large cell carcinoma
9	69	M	Bronchoscopy	Lower lobe	Oat cell carcinoma
10	67	F	Bronchoscopy	Middle lobe	Oat cell carcinoma
11	69	M	Lobectomy	Upper lobe	Adenocarcinoma
12	34	F	Cervical node	Mediastinum	Undifferentiated (unknown primary)

WD: well-differentiated; PD: poorly differentiated.

TABLE 2. ^{18}F FDG Uptake and Distribution Volumes for Tumor and Contralateral Lung Tissue

Patient	Mean tumor FDG uptake (ml/100 g/hr)	Maximum tumor FDG uptake (ml/100 g/hr)	Coefficient of variation (SD mean, %)	Contralateral lung FDG uptake (ml/100 g/hr)	Tumor distribution volume (ml/100 g)	Contralateral lung distribution volume (ml/100 g)
1	231.1	262.2	45.7	36.0	36.7	59.6
2	215.5	289.9	30.2	29.2	30.6	39.3
3	317.6	508.0	28.7	21.8	59.0	56.4
4	180.3	302.7	27.8	23.2	60.9	71.2
5	160.2	200.4	16.5	57.5	41.1	54.2
6	210.3	259.0	31.9	24.9	27.3	44.1
7	251.1	374.8	32.3	47.2	49.3	59.3
8	142.9	201.8	4.2	15.6	29.3	45.4
9	149.2	269.3	38.3	14.0	38.3	43.2
10	197.3	258.5	22.0	44.7	38.2	43.6
11	127.6	175.6	22.1	32.0	49.0	50.5
12	354.2	411.1	29.9	36.7	68.5	75.9
Means	211.4	292.9	30.5	31.9	44.0	53.1
SD	69.4	96.0	—	13.2	13.4	11.8

tumors have been the most thoroughly studied malignancies with respect to carbohydrate metabolism. Rhodes *et al.*¹⁶ measured ^{18}F FDG uptake in seven patients with cerebral gliomas. The overall ratio of uptake by tumor tissue to uptake by contralateral brain tissue was approximately 1.0. In a similar study Di Chiro *et al.*⁷ noted an increased maximum metabolic rate in 23 human gliomas compared with the white matter in 13 normal controls, although the tumor-to-gray matter ratio was only 1.04. Concerning other organs, Yonekura *et al.*⁸ measured ^{18}F FDG uptake in three patients with hepatic metastases from colonic carcinomas (although two had previously received chemotherapy). They reported a mean tumor-to-normal hepatic tissue ratio of 4.0. Therefore, the ^{18}F FDG uptake ratio of 6.6 for lung neoplasms is higher than either brain or liver tissue. This is probably because of the low rate of glucose consumption by normal pulmonary parenchymal tissue in the fasting state (0.3 mg glucose/100 g/min),¹⁰ which is less

than 10% of the metabolic rate of normal brain tissue. Assuming an equal fractional extraction ratio for ^{18}F FDG and glucose, then the mean metabolic rate for glucose in the lung tumors was 2.9 mg/100 g/min, which is still only half the metabolic activity of normal brain tissue.

The difference in the rates of ^{18}F FDG uptake between tumor and normal lung tissue indicate that ^{18}F FDG may be used to detect tumors, as suggested by Som *et al.*⁵ In their study of a variety of induced and transplanted tumors in animals, the tumor-to-normal tissue ratio for ^{18}F FDG uptake ranged from 2.1 to 9.1, which allowed the researchers to discriminate between malignant and nonmalignant tissue. In our study the mean ^{18}F fluorine activity per unit volume of thorax in the tumor tissue 1 hour after injection was 17.5 times that of normal lung. In addition, in the two patients with oat cell carcinoma increased ^{18}F FDG uptake was detected in separate areas adjacent to the tumor, which were consistent with enlarged lymph nodes on computerized tomograms. This

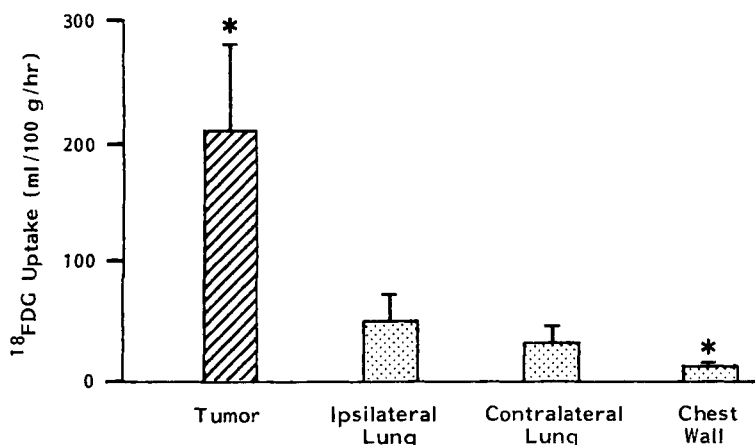
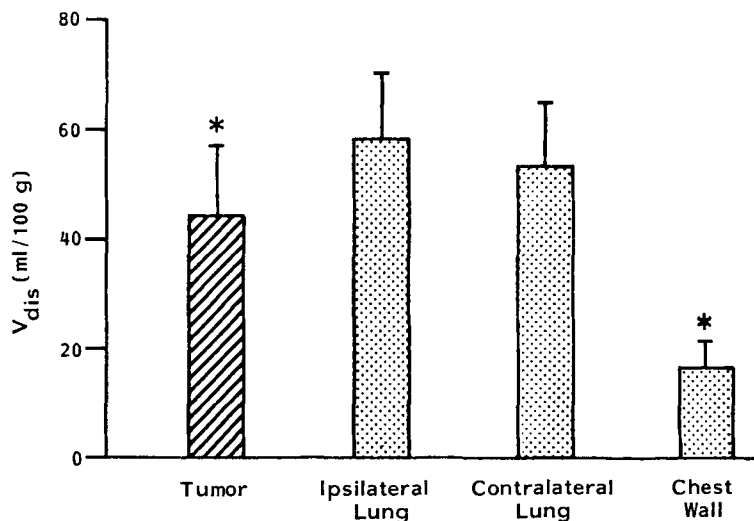


FIG. 3. Rates of ^{18}F FDG uptake (means \pm SD) for tumor, ipsilateral lung, contralateral lung, and chest wall (* $P < 0.05$).

FIG. 4. Calculated apparent volumes of distribution (means \pm SD) for tumor, ipsilateral lung, contralateral lung, and chest wall (* $P < 0.05$).



lends support to the technique for screening and staging purposes. However, one must be aware of other possible causes of ^{18}F FDG uptake, inflammation, for example,¹¹ and further studies are necessary to determine the specificity of ^{18}F FDG uptake by malignant tissue compared to nonmalignant diseases of the chest.

The other main finding of this study was that ^{18}F FDG uptake did not appear to correlate with the degree of differentiation of the tumor tissue. This contrasts with previous reports concerning other tissues. For example, in several experiments with tumors in animals¹ and in excised human tissue,¹⁷ the rate of glycolysis was reported to be higher in the more poorly differentiated tissue. Brain tumors in animals show a positive correlation between histologic grade and glucose uptake as assessed by ^{14}C -deoxyglucose autoradiography.¹⁸ Studies of brain tumors *in vivo* have also demonstrated that high-grade tumors exhibit visually distinct hot spots and have higher peak rates of ^{18}F FDG uptake.⁷

For lung tumors in particular, previous information on glucose metabolism is scanty. In the tissue culture study by Macbeth *et al.*¹⁷ only two lung tumors were reported; both were Grade III carcinomas with contrasting rates of anaerobic glycolysis. In the qualitative study by Suzuki *et al.*⁹ glucose uptake by four anaplastic carcinomas did not appear to differ from well-differentiated tumors. Of the six patients with lung carcinoma studied semiquantitatively by Fujiwara *et al.*,¹² the small cell carcinoma had the lowest rate of ^{18}F FDG uptake. In line with these findings, our results suggest that the degree of differentiation of lung carcinomas bears little relation to the rate of glucose utilization, even when expressed as maximum ^{18}F FDG uptake within the tumor slice. There were no striking qualitative differences in ^{18}F FDG uptake between well-differentiated and poorly differentiated tumors, nor were the rates of uptake qualitatively dis-

similar. Lung tumors may indeed differ from liver and brain tumors in the enzymatic or membrane transport changes accompanying the loss of differentiation. Alternatively, since most of the histologic samples were small, and the metabolic activity within each tumor slice was usually heterogenous, histologic-metabolic correlations may have been missed. In addition, an image resolution of 1.7 cm full-width half-maximum may have rendered our PET scanner relatively insensitive to scattered small areas of necrosis. If the more aggressive tumors had multiple small areas of necrosis, the rate of ^{18}F FDG uptake by viable tumor tissue may have been higher than the overall measured rate.

An unexpected finding of this study was the difference in the rates of ^{18}F FDG uptake between the two lungs within the slice. Not all the patients showed this pattern, but the mean ipsilateral lung uptake was 1.5 times the rate of uptake by the contralateral lung. It is possible that the lung tissue near the tumor was infiltrated by an inflammatory process (with increased ^{18}F FDG uptake by phagocytic cells) or subclinical tumor, both of which could cause an increased rate of glucose consumption. More likely, however, an unapparent photon spillover from the adjacent tumor may have falsely raised the measured ^{18}F FDG uptake in the ipsilateral lung tissue. Nevertheless, it is interesting to compare this finding with observations made in patients with brain tumors using similar methodology. In contrast to our findings, Di Chiro *et al.*⁷ and De La Paz *et al.*¹⁹ noted a regional depression of glucose utilization in adjacent cortical regions or areas neurally connected to the tumor. This was attributed to peritumoral edema or tumor-associated cortical suppression. Lung tissue, however, is structurally very different from brain tissue and is less susceptible to the pressure effects of a space-occupying lesion.

Because the calculated apparent volume of distribu-

TABLE 3. Key to Symbols

$C_{WB}(t)$	Whole blood ^{18}F concentration at time t ($\mu\text{Ci}/\text{ml}$)
$C_p(t)$	Plasma ^{18}F concentration at time t ($\mu\text{Ci}/\text{ml}$)
V_B	Measured regional blood volume ($\text{ml blood}/\text{cm}^3$ thorax)
$C_{EV}(t)$	Extravascular ^{18}F concentration at time t ($\mu\text{Ci}/\text{g}$ extravascular tissue)
D_{EV}	Extravascular lung density ($\text{g extravascular tissue}/\text{cm}^3$ thorax)
$C_f(t)$	Extravascular free (nonphosphorylated) ^{18}F concentration at time t
$C_m(t)$	Extravascular metabolized (phosphorylated) ^{18}F concentration at time t
V_{dis}	Apparent distribution volume for free (nonphosphorylated) ^{18}F (ml/g extravascular tissue)
E	Arteriovenous extraction fraction for ^{18}F
Q_{EV}	Flow per unit extravascular tissue mass ($\text{ml}/\text{g}/\text{min}$)

tion for ^{18}F in normal lung tissue is low (10), an increase in uptake must depend primarily upon increased transport of ^{18}F from the interstitium into the cells. In each patient in this study the apparent volume of distribution for ^{18}F within the tumor tissue (which includes both extracellular and intracellular compartments) was less than the value for the contralateral normal lung tissue. A more definitive assessment of glucose transport into the tumor cells would require an accurate measurement of extracellular *versus* intracellular volume. However, because the calculated overall tissue concentration of nonphosphorylated ^{18}F is low, the cellular concentration must also be low; this implies that cellular transport into lung tumor tissue is the rate-limiting step for glucose uptake, just as in normal lung tissue.

The measurement of glucose metabolism in lung tumors has several potential clinical applications. For example, the high rate of ^{18}F uptake allows us to distinguish neoplastic from normal lung tissue, and conceivably has a role in defining the extent of viable tumor. Although not as anatomically discriminating as radiography or computerized tomography, PET scanning gives a direct measurement of the metabolic activity of neoplastic tissue, thereby providing physiological resolution to augment the anatomic resolution of conventional radiologic procedures.

More importantly, serial measurement of a tumor's metabolic activity should enable a more definitive assessment of the response to conventional therapy, leading perhaps to the development of alternative drugs specifically tailored to the tumor's hexokinase activity. The analogue 2-deoxyglucose itself, in combination with antimetabolic agents, is currently being studied as therapy in experiments on animal tumors.²⁰ In non-small cell lung tumors, for which conventional nonsurgical therapy is so poor, selective metabolic inhibitory agents may hold considerable promise.

APPENDIX

In formulating this model, the following assumptions were made (key to symbols is shown in Table 3):

1. The region of lung tissue under study is in a physiologic steady state and is therefore metabolizing glucose at a constant rate.
2. Ten minutes after the intravenous injection of ^{18}F , the extravascular tissue concentration of free (nonphosphorylated) ^{18}F (which comprises intracellular and extracellular moieties) is in dynamic equilibrium with the capillary plasma concentration.
3. Once within the cell, ^{18}F is phosphorylated by hexokinase at a rate dependent on the metabolic activity of the enzyme, and that there is no significant leak of the labeled phosphate out of the cell or hydrolysis of the phosphate bond.
4. The plasma concentration [$C_p(t)$] and whole blood concentration [$C_{WB}(t)$] of ^{18}F in tissue capillaries of tumor and normal lung are equal to the concentrations in peripheral venous blood.

The reconstructed tomogram of ^{18}F activity represents the quantitative distribution of isotope per unit volume of thorax (*i.e.*, $\mu\text{Ci}/\text{cm}^3$ thorax). Part of this signal arises from free ^{18}F within the pulmonary vascular pool and must therefore be subtracted. This background is calculated as $C_{WB}(t)V_B$, where $C_{WB}(t)$ is the ^{18}F concentration in whole blood at time t , and V_B is the measured regional blood volume for lung or tumor ($\text{ml blood}/\text{cm}^3$ thorax). The remaining (extravascular) thoracic content of activity is converted into extravascular tissue concentration [$C_{EV}(t)$ in units of $\mu\text{Ci}/\text{g}$ of EV tissue] by dividing by the regional distribution of extravascular lung density [(D_{EV}) in units of g/cm^3 thorax]. $C_{EV}(t)$ can be considered to be made up of two components—free ^{18}F [$C_f(t)$] and ^{18}F that has been metabolized to phosphate [$C_m(t)$]. Thus

$$C_{EV}(t) = C_f(t) + C_m(t) \quad (1)$$

The relationship between $C_f(t)$ and $C_p(t)$ can be considered in terms of an apparent distribution volume V_{dis} (see assumption 2) where

$$C_f(t) = V_{dis}C_p(t) \quad (2)$$

Since $C_f(t)$ has the units of $\mu\text{Ci}/\text{g}$ tissue and $C_p(t)$ has units of $\mu\text{Ci}/\text{ml}$ plasma, then V_{dis} has units of $\text{ml plasma}/\text{g tissue}$.

The metabolic accumulation of tissue ^{18}F at any given time t [$C_m(t)$] is proportionate to the following:

1. The capillary whole blood concentration of ^{18}F at that time
2. The steady state extraction fraction (E) for ^{18}F
3. The flow per unit extravascular mass (Q_{EV}) of the tissue

Therefore, an incremental increase in tissue concentration [$C_m(t)$] can be expressed in terms of these parameters by the equation

$$\Delta C_m(t) = Q_{EV}E C_{WB}(t) \Delta t \quad (3)$$

where Δt is a short time period. Integration of this equation to time T yields

$$C_m(T) = Q_{EV}E \int_0^T C_{WB}(t) dt \quad (4)$$

Incorporating equations 2 and 4 into equation 1 and dividing all terms by $C_p(T)$ gives

$$\frac{C_{EV}(T)}{C_p(T)} = V_{dis} + Q_{EV}E \frac{\int_0^T C_{WB}(t) dt}{C_p(T)} \quad (5)$$

Plotting the tissue-to-plasma concentration ratio [$C_{EV}(T)/C_p(T)$] against the ratio of integrated whole blood concentration to plasma concentration [$\int_0^T C_{WB}(t) dt / C_p(T)$] at various times T results in a linear function where the slope = $Q_{EV}E$ for ^{18}F , which quantifies the rate of ^{18}F uptake. The intercept = V_{dis} for ^{18}F , which is the apparent (relative) distribution volume.

REFERENCES

1. Warburg O. On the origin of cancer cells. *Science* 1956; 123:309-314.
2. Hatanaka M. Transport of sugars in tumor cell membranes. *Biochem Biophys Acta* 1974; 355:77-104.
3. Weber G. Enzymology of cancer cells (part 2). *N Engl J Med* 1977; 296:541-555.
4. Sokoloff L, Reivich M, Kennedy C *et al.* The ¹⁴C-deoxyglucose method for the measurement of local cerebral glucose utilization: Theory, procedure, and normal values in the conscious and anesthetized albino rat. *J Neurochem* 1977; 28:897-916.
5. Som P, Atkins HL, Bandyopadhyay D *et al.* A fluorinated glucose analog, 2-fluoro-2-deoxy-D-glucose (F-18): Nontoxic tracer for rapid tumor detection. *J Nucl Med* 1980; 21:670-675.
6. Fukuda H, Matsuzawa T, Abe Y *et al.* Experimental study for cancer diagnosis with positron-labelled fluorinated glucose analogs. *Eur J Nucl Med* 1982; 7:294-297.
7. Di Chiro G, DeLaPaz RL, Brooks RA *et al.* Glucose utilization of cerebral gliomas measured by (¹⁸F) fluorodeoxyglucose and positron emission tomography. *Neurology* 1982; 32:1323-1329.
8. Yonekura Y, Benua RS, Brill AB *et al.* Increased accumulation of 2-deoxy-2-(¹⁸F)-fluoro-D-glucose in liver metastases from colon carcinoma. *J Nucl Med* 1982; 23:1133-1137.
9. Suzuki T, Iio M. The clinical application of ¹¹C-glucose for diagnosis of lung cancer. Proceedings of Third World Congress of Nuclear Medicine and Biology 1982; 2080-2082.
10. Rhodes CG, Valind SO, Brudin L *et al.* Modulation of pulmonary glucose utilization by dietary state in man (Abstr). *Clin Sci* 1985; 68:21.
11. Valind SO, Rhodes CG, Pantin C, Suzuki T, Hughes JMB. Measurement of pulmonary glucose metabolism in patients with cryptogenic fibrosing alveolitis and pulmonary sarcoidosis (Abstr). *Am Rev Respir Dis* 1984; 129:353.
12. Fujiwara T, Matsuzawa T, Ito M *et al.* F-18-deoxy-D-glucose positron emission tomography of human lung tumors. Cyclotron and Radioisotope Center Annual Report 1984; 264-269.
13. World Health Organization: The World Health Organization histological typing of lung tumors. *Am J Clin Pathol* 1982; 77:123-136.
14. Rhodes CG, Wollmer P, Fazio F, Jones T. Quantitative measurement of regional extravascular lung density using positron emission and transmission tomography. *J Comput Assist Tomog* 1981; 5:783-791.
15. Brudin LH, Valind SO, Rhodes CG, Turton DR, Hughes JMB. Regional lung hematocrit in humans using positron emission tomography. *J Appl Physiol* 1986; 60:1155-1163.
16. Rhodes CG, Wise RJS, Gibbs JM *et al.* *In vivo* disturbance of the oxidative metabolism of glucose in human cerebral gliomas. *Ann Neurol* 1983; 14:614-626.
17. Macbeth RAL, Bekesi JG. Oxygen consumption and anaerobic glycolysis of human malignant and normal tissue. *Cancer Res* 1962; 22:244-248.
18. Yamada K, Hayakawa T, Ushio Y *et al.* Regional blood flow, capillary permeability, and glucose metabolism in the rat with ethylnitrosourea-induced rat glioma. *J Cerebral Blood Flow* 1981; (Suppl) 1:S571-572.
19. DeLaPaz RL, Patronas NJ, Brooks RA *et al.* Positron emission tomography study of suppression of gray-matter glucose utilization by brain tumors. *Am J Nuc Rad* 1983; 4:826-829.
20. Bernal SD, Lampidis TJ, McIsaac RM, Chen LB. Anticarcinoma activity *in vivo* of Rhodamine 123, a mitochondrial-specific dye. *Science* 1983; 222:169-172.